

AD650740

4168.13-2

B2130-T-11

SEMI-ANNUAL TECHNICAL REPORT

1 OCTOBER 1966 - 31 MARCH 1967

ARPA ORDER NO 462  
ARPA PROGRAM CODE NO. 3950  
ARO-D-PROJECT NO. 4168\*  
CONTRACT NO. DA-31-124-ARC(D)-142  
THE FRANKLIN INSTITUTE RESEARCH LABORATORIES  
CHEMISTRY DEPARTMENT

Distribution of this document is unlimited.

The findings in this report are not to be construed as an official  
Department of the Army position, unless so designated by other  
authorized documents.

DIFFUSION IN ORGANIC CRYSTALS

ARCHIVE COPY

D D C  
APR 28 1967  
FBI - PHILADELPHIA



THE FRANKLIN INSTITUTE RESEARCH LABORATORIES

**BEST  
AVAILABLE COPY**

SYNOPSIS

Further self-diffusion studies have been carried out on anthracene crystals at high temperature. A comparison has been made between crystals grown from the vapor, the melt and commercially supplied melt-grown crystals in which it was found that the secondary or fast diffusion process increased in the order vapor-grown < melt-grown < commercial melt-grown. The bulk diffusion coefficients for the vapor and melt-grown crystals were also significantly lower than for the commercially supplied crystals. No correlation could be found between diffusion coefficients and dislocation densities or charge carrier lifetimes.

A thorough investigation has been made into the purity and perfection of a large melt-grown anthracene crystal. Segregation coefficients have been obtained for hole and electron traps introduced by thermal decomposition in the melt.

An exhaustive study has been made on the growth of anthracene crystals from the vapor phase as a function of purification technique, ambient growth atmosphere, growth temperature, supersaturation and the effect of light. Crystals have initially been evaluated by carrier lifetime measurements from which it has been found that the best growing conditions are purification by combination tube growth under  $\sim$  1-2 mm inert gas at a temperature of 120-140°C under red light. The best crystals obtained by this technique, however, gave carrier lifetimes a factor of 5 lower than the best melt-grown crystals, though diffusion studies indicate

that they have the lowest self-diffusion coefficient.

~~Fig. 1~~ An attempt has been made to examine the physical substructure of anthracene by electron microscopy. Surface replicas have been photographed for crystals grown under different conditions and in one instance an anthracene crystal has been photographed under high magnification.

## I. DIFFUSION STUDIES

Work in this field has been confined to two topics.

1. A comparison of self-diffusion in high purity melt-grown anthracene crystals, high purity sublimation-grown anthracene crystals and melt-grown crystals supplied by the Harshaw Chemical Company.
2. Further studies on hydrogen diffusion through anthracene crystals grown from the melt, and by sublimation, as a function of temperature.

### 1. SELF-DIFFUSION STUDIES

Two important aspects of the self-diffusion studies are the effect of purification and method of crystal growth. Until recently all our results on self- and impurity-diffusion in anthracene have been obtained on commercially supplied melt-grown single crystals as our own crystal growing facility was being developed during the preceding phase of the program. Previous reports have included measurements of purity, electrical properties and physical structure of our own crystals but it has only been recently that crystals of suitable size for self-diffusion studies have been available.

A series of carefully controlled self-diffusion studies have been carried out on anthracene crystals which have been a) melt-grown b) vapor-grown and c) commercially supplied melt-grown. All crystals were identically prepared by benzene polishing on fine lens paper. This polishing procedure results in a microscopically roughened surface which from etching studies was found to be less than 5-10  $\mu$  thick. Three batches of crystals were selected which contained at least one crystal from each group a), b) and c). All the crystals in each batch were prepared for the diffusion anneal

by flash evaporation of  $C^{14}$ -anthracene simultaneously under high vacuum ( $10^{-5}$  mm Hg). Each crystal was individually wrapped with aluminum foil to prevent evaporation and to ensure uniform temperature distribution around the crystal. Each batch of crystals was then placed in a glass tube, pumped under high vacuum for at least 1 hour and sealed off in the minimum volume under a "Purgon" atmosphere calculated to give 1 atmosphere pressure at the anneal temperature.

Three batches of crystals were diffusion annealed in the same oven at  $191.0^{\circ}C \pm 0.5^{\circ}C$  and batches were removed after 168 hrs, 425 hrs and 696 hrs.

To date only the first batch has been analyzed and the penetration profiles obtained are shown in Figure 1. In this graph all curves have been normalized to 1 sq. mm of surface area per 7 micron thick section.

The factor immediately obvious from this graph is the variation in the secondary diffusion process in which the penetration for both vapor-grown crystals < melt-grown crystal << commercial melt-grown crystal.

The bulk diffusion process, on the other hand, is much smaller than expected from previous measurements at this temperature,  $\sim 4 \times 10^{-12} \text{ cm}^2 \text{ sec}^{-1}$ . (1) This smaller penetration resulted in less accurate bulk diffusion coefficients. Bulk diffusion coefficients were calculated after subtracting the secondary process, and are included in Table I. The secondary diffusion process also appears linear in Figure 1 and the relative penetration has been included in Table I as the relative

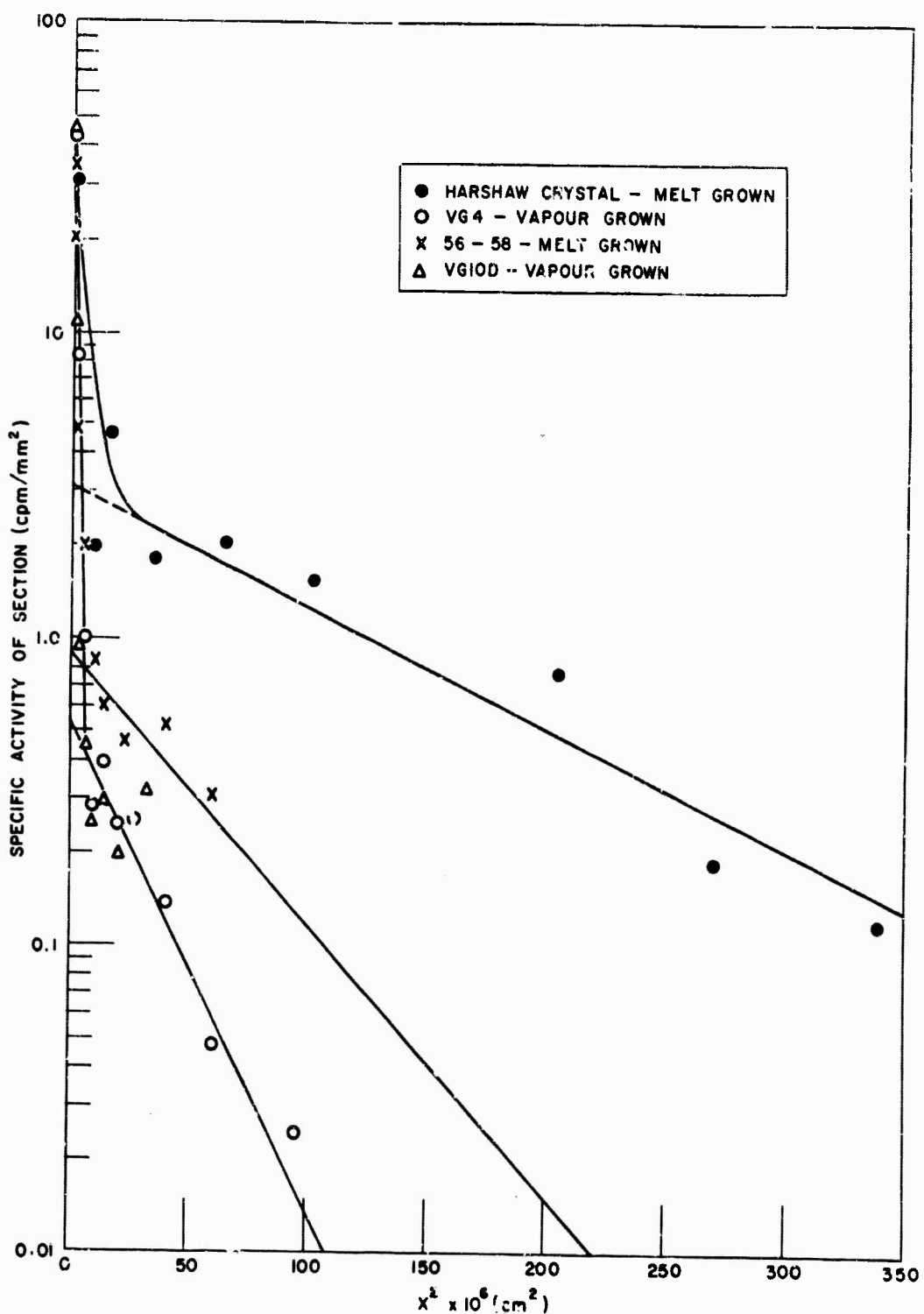


FIGURE 1. Penetration Profiles for Self-Diffusion Perpendicular to 001 Plane in Anthracene at 190°C, After 168 Hour Anneal.

TABLE I

<u>Crystal Symbol</u>	<u>Bulk Diffusion Coefficient, <math>D_B</math> <math>\text{cm}^2 \text{ sec}^{-1}</math></u>	<u>Relative Penetration of Secondary Process</u>	<u>Dislocation Density, <math>\text{cm}^{-2}</math></u>	<u>Hole Carrier Lifetime</u>	
				<u>Before Diffusion <math>\mu\text{s}</math></u>	<u>After Diffusion <math>\mu\text{s}</math></u>
VG4	$6.5 \times 10^{-13}$	.25	$1.5 \times 10^6$	15-20	19
VG10D	$3.0 \times 10^{-13}$	.25	$9 \times 10^5$	35-45	50-60
56-58	$5.0 \times 10^{-13}$	.45	$2.7 \times 10^6$	400-500	130-140
Harchaw	$\sim 2 \times 10^{-12}$	1.0	$1.5-3.0 \times 10^5$	(50-100)	60-70

reciprocal line gradient.

Both before and after diffusion anneal, measurements of the dislocation density and "hole" charge carrier trapping lifetime were carried out. These are included in Table I.

From this table several important features can be noted.

1) There is no apparent correlation between the bulk diffusion coefficient or the secondary diffusion process and the dislocation density and indeed the highest diffusion coefficient is associated with the lowest measured dislocation content. This result suggests that the secondary process is not due to diffusion down this particular line defect system.

2) There is no correlation between either diffusion process and the hole carrier lifetime.

3) The effect of annealing on the carrier lifetime was not significant for the vapor-grown or Harshaw crystals but reduced that of the melt-grown crystal by a factor of 3.

4) Both bulk and secondary diffusion processes appear correlated in that a large  $D_B$  is associated with a higher background penetration.

5) The bulk diffusion coefficient of the commercial melt-grown crystal is in fair agreement with the value previously found at this temperature<sup>(1)</sup> but is a factor of 3 larger than either the melt- or vapor-grown crystals. In view of the non-dependence of diffusion on the dislocation content this suggests that the controlling factor is either chemical purity as both melt- and vapor-grown crystals were extensively

purified or another type of physical defect which does not show up with this etching technique.

6) Another important point illustrated by these measurements is the confirmation of the low diffusion coefficient previously obtained on annealing at high temperatures<sup>(1)</sup>. These results suggest that some type of defect annealing can take place in anthracene with an onset temperature of around 190°C. This result is identical to that found in naphthalene by Sherwood and White<sup>(2)</sup>.

Of great interest, therefore, will be the results of longer anneal times at this temperature which may show a time dependent diffusion coefficient if defect annealing is occurring at a significant rate in the bulk crystal.

## 2. TRITIUM DIFFUSION THROUGH ANTHRACENE

Work on this section of the program has continued with measurement of the temperature variation of the permeability and diffusion constant made possible by starting the experiments at different temperatures.

Unfortunately results have been obtained which are a factor of ten or more lower than the original values. These results, however, have all been obtained using a second batch of tritium gas and it is felt that the results reflect the differences in the batches. Quantitative measurements of a specific activity indicate that the batches have the stated specific activity. Both batches differed considerably in their initial specific activity as delivered. The first batch had a specific activity of 60,000 millicuries/millimole and was diluted by us. The second batch was supplied at 25 mc/millimole.

A third batch of tritium has been ordered and it is intended to repeat the original measurements. Hence this phase of the work will be reported in the next report when these problems have been resolved.

## II. DEFINITION AND ATTAINMENT OF PURITY AND PERFECTION IN ORGANIC CRYSTALS

Studies have continued in this area, the emphasis being placed on elucidating the role of impurities, ambient conditions, and physical defect structure on charge carrier generation and trapping processes in organic crystals. Transient photoconduction studies have been carried out on carefully grown anthracene crystals obtained from the melt and the vapor phase. To supplement these investigations and aid in interpretation of the data, studies have continued on dislocation etching and a study of anthracene crystals by means of electron microscopy has been initiated.

### 1. STUDIES ON MELT-GROWN ANTHRACENE CRYSTALS

An attempt has been made to study the effect of growth rate on the physical properties of melt-grown anthracene crystals. For this investigation a long crystal 11 cm x 1.5 cm dia. was grown in a Bridgman oven such that three sections of the crystal were grown at different rates. The first 3 cm was grown at  $0.77 \text{ mm hr}^{-1}$ , the second 3.5 cm at  $1.9 \text{ mm hr}^{-1}$  and the remaining 4.5 cm of the crystal grown at  $3.5 \text{ mm hr}^{-1}$ .

The crystal grew with a vertical cleavage plane with the "b" direction vertical. The appearance of the crystal on removal from the oven was excellent with the exception that a trace of a brown substance could be observed at the very top of the crystal. This was due to thermal decomposition of the anthracene in the melt caused by the crystal growing tube extending into the hottest region of the oven. Here it was exposed to temperatures of  $240-250^\circ\text{C}$  for a 3 day period prior to growth as the

crystal had to be restarted because of poor initiation.

The three regions of differing growth rate were carefully cut out and samples of each from accurately measured positions in the boule were examined by carrier lifetime studies for both hole and electron pulses. Two series of measurements were made on these crystals. The variation in carrier lifetime along the boule was measured and the variation in carrier lifetime was measured across the crystal at constant height.

This crystal proved to be extremely informative and the more important findings were as follows.

Excellent photocurrent transient pulses were obtained for all crystals for both hole and electron injection. The principle features of these pulses are illustrated graphically for crystal section 1-3 which was taken from the purest part of the boule.

Figure 2 shows the current-voltage characteristics for both electron and hole pulses. As has been done with previous crystals the boule was broken open in a Purgeon purged glove box and the crystal was measured first in a Purgeon atmosphere then in air to observe any surface/ambient gas effect. In this crystal the only effect was to increase the carrier generation efficiency for holes without altering the carrier lifetime. This was similar to previous measurements<sup>(3)</sup>. The fact that there was no reduction in carrier lifetime may be due to the increased impurity content of this crystal caused by prolonged exposure to temperatures  $> 300^{\circ}$  above the melting point. Previously the reduction in carrier lifetime had been observed only with crystals having initial lifetimes over 1 millisecond whereas this crystal had an initial lifetime of 300  $\mu$ s.

In Figure 2, it can be seen that the characteristics of

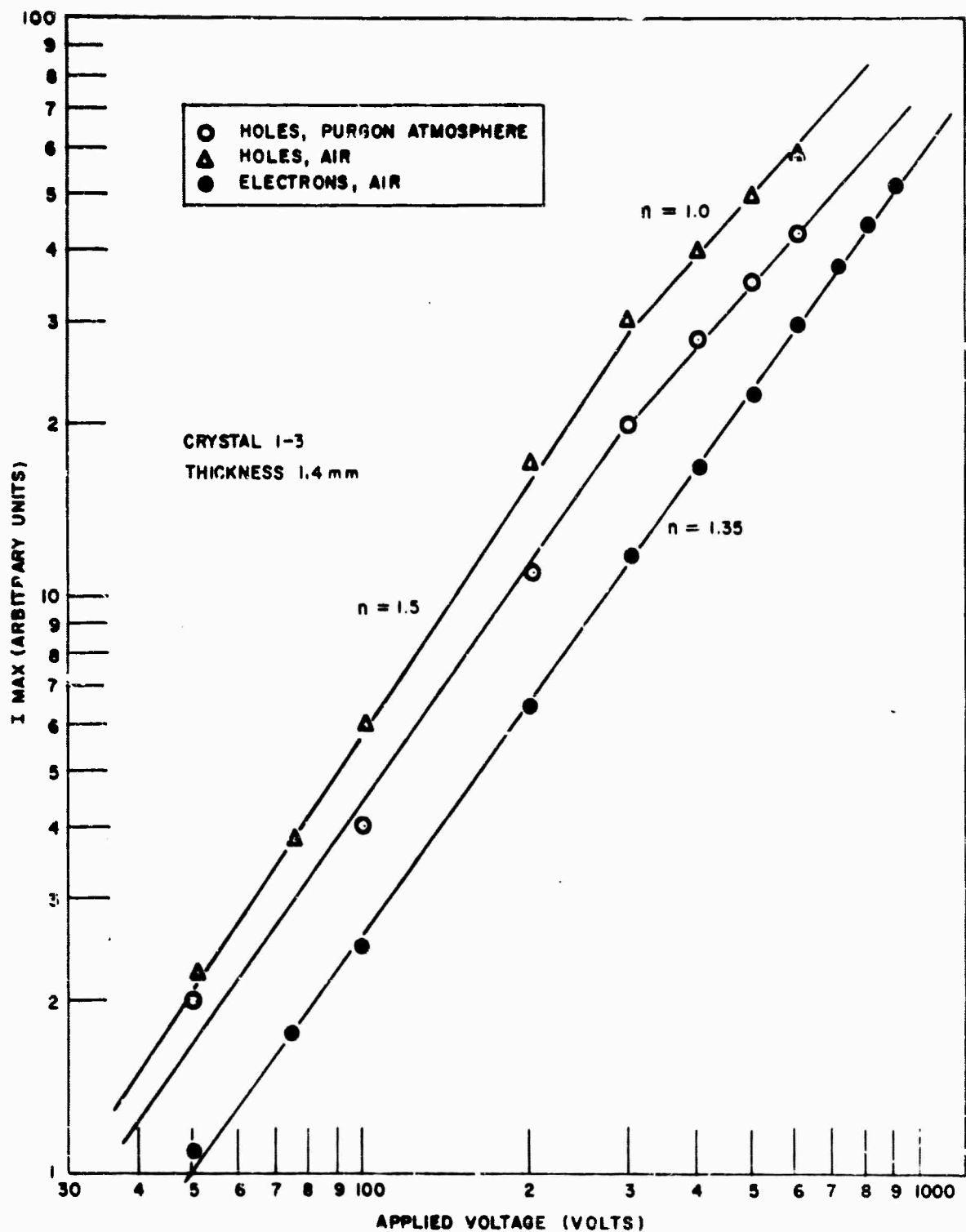
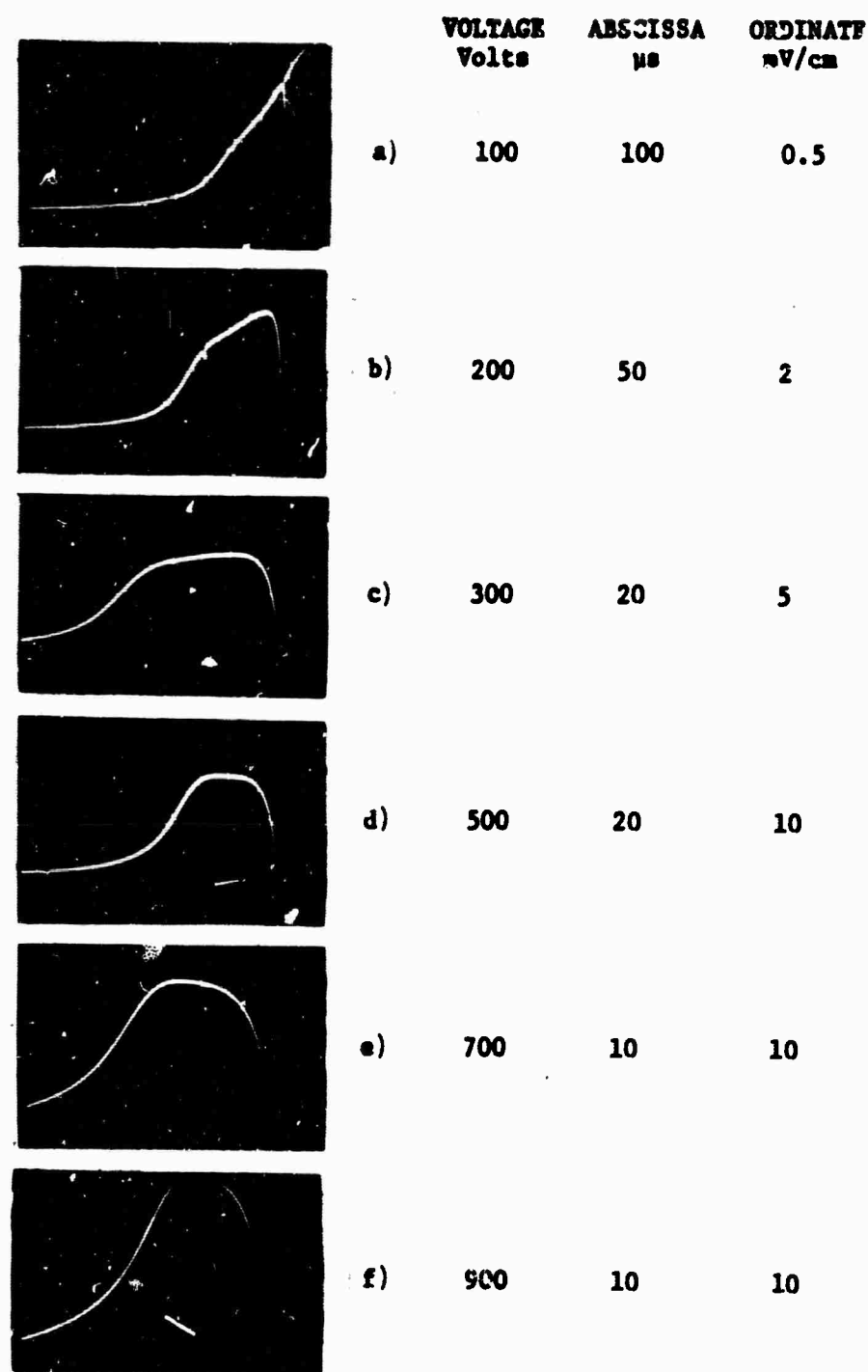


FIGURE 2. Current-Voltage Characteristic of "Hole" and Electron Photocurrents for Anthracene Crystal 70-62, section 1-3.

holes and electrons are different. The hole characteristic has a distinct break in the curve at 300 volts whereas the electron current has none. It was also observed that at the onset of this break the carrier lifetime began to change. A series of hole pulses with increasing applied voltage are shown in Figure 3. Below the break the carrier lifetime is constant but above the break a second effect sets in in which the pulse shape continually changes until it has the appearance of a space charge limited pulse. This, however, cannot be the case as the hole mobility is invariant through the transition (see Figure 4) and the light intensity dependence of the current is also constant, the current being directly proportional to intensity, see Figure 5. Both these effects characterize space charge free behavior and agree with experimental observations of Castro<sup>(4)</sup> who also observed pulses similar to our high voltage pulse. These were only found, however, in air exposed crystals using long wavelength light (394  $\mu$ ) i.e. conditions almost identical to ours. His explanation was that it was due to an extrinsic hole generation process. In our experiments we have found that this behavior is only field dependent and is not appreciably dependent on ambient gas.

Below the break in the I-V curve both holes and electrons have almost the same characteristic,  $I_a(V)^n$  where  $n_+ = 1.5$ ,  $n_- = 1.35$ , and the  $I_{max}$  values differ only by a factor of 2. It seems reasonable to suggest that the intrinsic charge generation mechanism is the same for both holes and electrons but that exposing the crystal surface to air affects the charge generation efficiency of holes only.

For both holes and electrons it was found that the carrier lifetime of each was independent of voltage over a large voltage range,



**FIGURE 3. Anthracene Photocurrent "Hole" Transient Pulses as a Function of Applied Voltage.**

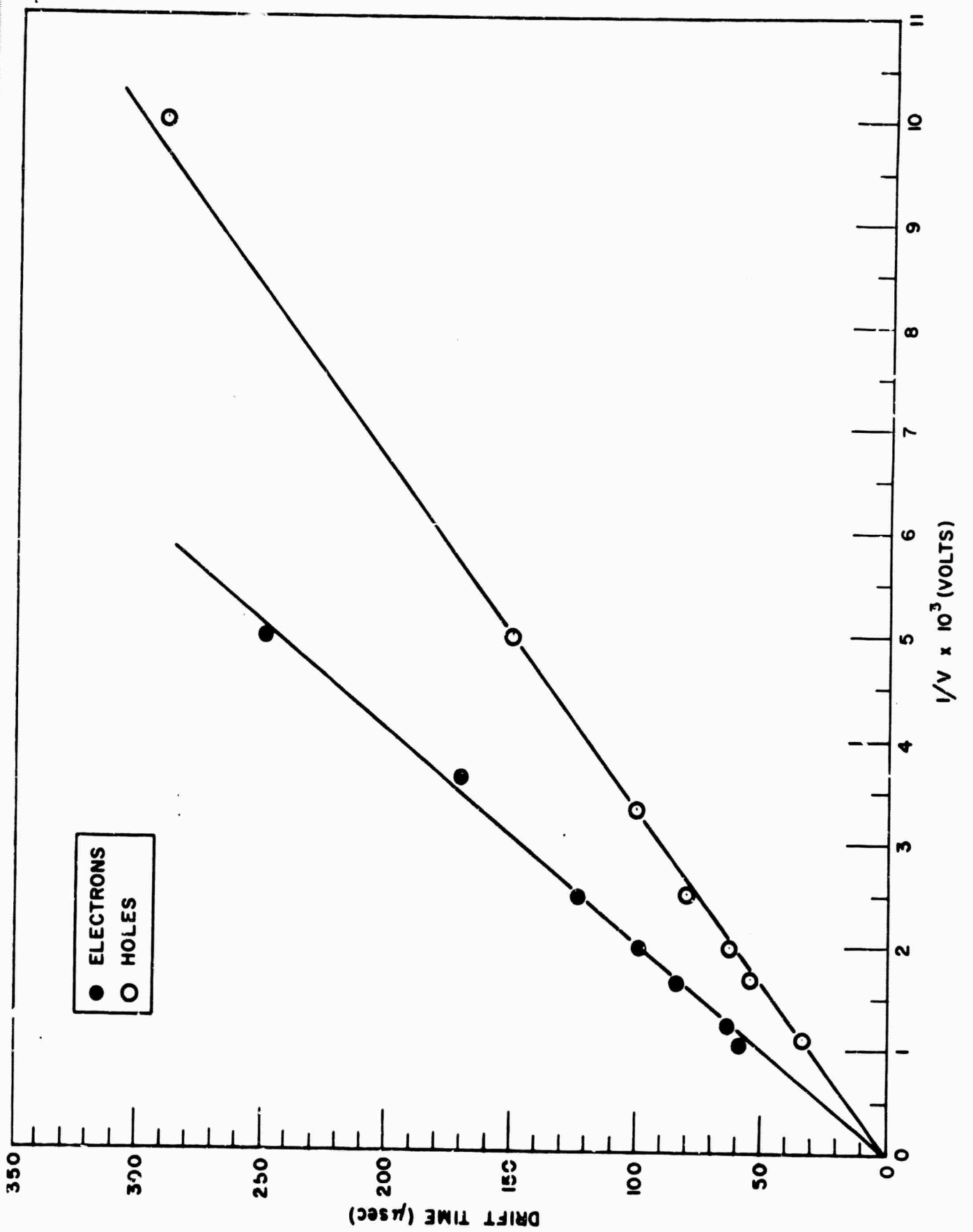
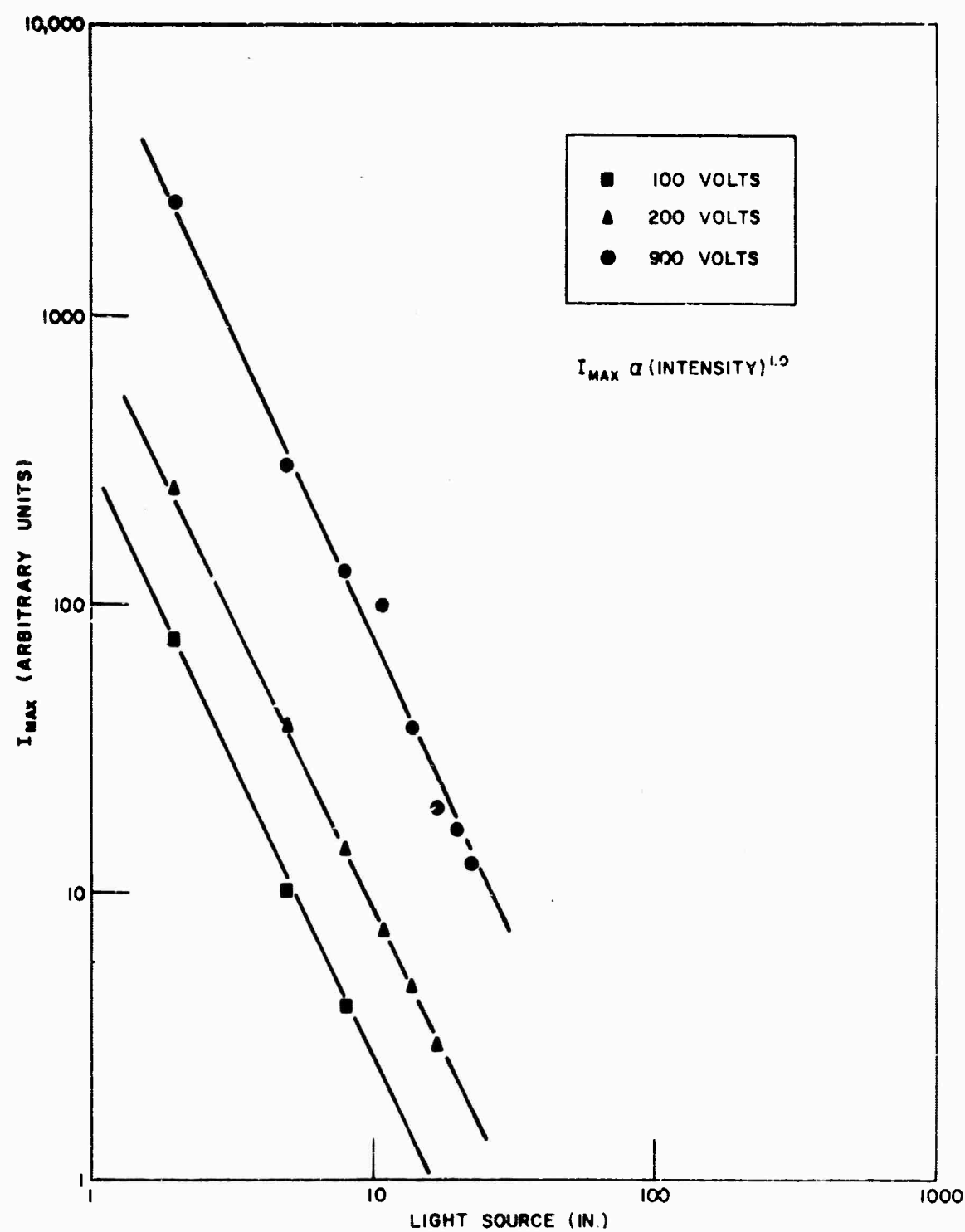


FIGURE 4. A Plot of Drift Time Vs. Reciprocal Voltage for Anthracene  
Crystal 70-62/1-3.



**FIGURE 5. Dependence of Photocurrent on Light Intensity as a Function of Applied Voltage.**

50-200 V for holes and 50-900 V for alactrons. Hence lifetimes have only been quoted where they are constant over a large range of applied voltage. All carrier lifetime and mobility data obtained on this crystal are summarized in Table II.

For electron traps the following relation holds<sup>(5)</sup>

$$\sigma = \frac{1}{N_t \tau_c v}$$

where  $N_t$  is density of trapping centers,  $\tau_c$  the trapping lifetime,  $v$  the thermal velocity of the electrons and  $\sigma$  the capture cross section. Hence the trap density is inversely proportional to carrier lifetime. A similar expression holds for hole traps even in the case of shallow trapping where the following expression holds.

$$\frac{\tau_c}{\tau_r} = \frac{N_c}{N_t} \exp - \frac{E_t}{R1}$$

where  $\tau_r$  is the trap release time,  $N_c$  the effective density of states in the carrier band of interest and  $E_t$  the energy separation between trap and carrier band. Hence the relative distribution of hole and electron traps in the crystal boule is known if the variation in lifetime is known.

If the electron and hole traps are chemical impurities which segregate out of the crystal on single crystal growth then their segregation coefficient should obey the classical expression for directional freezing<sup>(6)</sup>.

TABLE II

## PHOTOCURRENT TRANSIENT DATA FOR ANTHRACENE CRYSTAL 70-62

Crystal Symbol	Position in Boule From Bottom cm	Carrier Lifetime		Carrier Mobility		$\frac{\tau_h}{\tau_e}$	1-g
		Hole μs	Electron μs	$\frac{\text{cm}^2 \text{ sec}^{-1} \text{ v}^{-1}}{\text{Hole} \text{ μs} \text{ Electron} \text{ μs}}$			
7-8	10.0	90-105	42-48	0.62	0.31	2.16	.10
9-8	9.0	120	—	—	—	—	—
6-8	9.0	80-95	50	0.58	0.33	2.05	.18
5-8	9.0	105	56-58	0.80	0.38	1.75	.18
4-8	9.0	95-110	50-52	0.64	0.34	1.95	.18
8-8	9.0	100-120	—	—	—	—	.18
2-8	8.0	140-155	58-68	~ 0.65	—	2.35	.27
3-8	7.0	140-155	—	0.67	—	—	.36
1-8	7.0	175-195	105-120	0.60	0.35	1.65	.36
5-6	5.5	220-250	—	—	—	—	.50
1-6	5.0	135-145	78	0.755	0.20	1.8	.55
2-6	5.0	110-130	72-92	0.50	0.25	1.5	.55
3-6	5.0	140	68	0.755	—	1.6	.55
4-6	4.5	210-240	135-150	0.73	—	—	.59
1-3	3.0	260	220-235	0.765	0.45	1.18	.73
2-3	3.0	280	190	0.78	0.37	1.47	.73
4-3	2.0	260-290	200	0.72	0.38	1.37	.82
3-3	1.0	292-300	—	0.74	—	—	.91

$$c/C_0 = k (1-g)^{k-1}$$

where  $C_0$  is the initial concentration of the impurity in the melt,  $c$  is the concentration at the point where a fraction  $g$  of the crystal has solidified and  $k$  is the segregation coefficient.

Figure 6 shows a plot of  $\log$  (reciprocal carrier lifetime) vs  $\log (1-g)$  where  $g$  is the fraction of the boule solidified, for both electron and hole traps.

As the initial impurity concentration  $C_0$  is unknown we can obtain the segregation coefficients for electron traps and hole traps only from the line gradient. These were found to be.

$$k_{\text{hole trap}} = 0.42$$

$$k_{\text{electron trap}} = 0.15$$

It is believed that these impurities were solely due to thermal degradation in the melt for several reasons. Other melt-grown crystals which had been purified and grown under identical conditions gave lifetimes which were a factor of 3-4 greater, the only difference being that they were held in the melt for a much shorter time. Also if these impurities had been present in the original material, then the zone refining procedure should have reduced their concentration to a very low level, especially the electron trapping impurity whose segregation coefficient is 0.15.

It is also apparent from Figure 6 that the segregation of these impurities is unaffected by growth rates in the range 0.77 mm/hr<sup>-1</sup> to 3.5 mm hr<sup>-1</sup>. The distribution of points around the lines in Figure 6

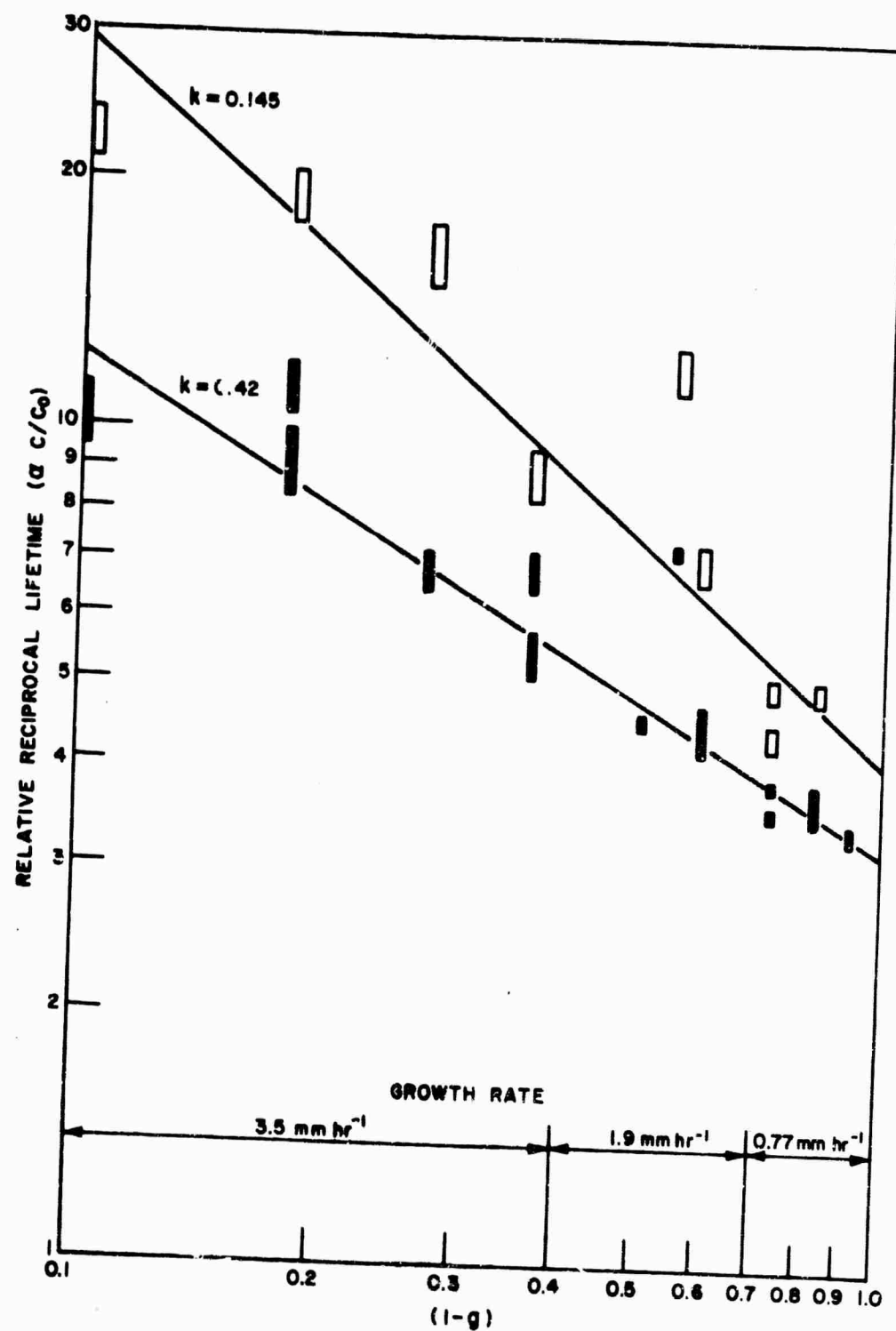


FIGURE 6. Segregation Plot for Impurities in Anthracene Crystal 70-62-1-3.

is a common effect found when directional freezing experiments are performed in unstirred vessels<sup>(7)</sup>.

Measurement of the dislocation density in this crystal yielded very interesting results. The dislocation density was found to be initially high at the purest part of the boule and decrease towards the top. Typical values were  $3 \times 10^6 \text{ cm}^{-2}$  at the bottom,  $2 \times 10^6 \text{ cm}^{-2}$  in the middle and  $6-10 \times 10^5 \text{ cm}^{-2}$  at the top of the boule. The etch patterns were more difficult to observe at the top of the boule probably due to chemical impurities interfering with the etching process.

These results are unusual in that

- 1) Increasing the impurity content would be expected to increase the dislocation concentration due to increasing stress in the crystal.
- 2) Increasing the growth rate would also be expected to give the same effect as this would give an effectively sharper temperature gradient which should lock in dislocations by giving them less time to anneal out. The large dislocation density of the boule is not unique as the same dislocation density was found in a previous melt-grown crystal, ref. 56-58, which gave even longer carrier lifetimes. It would appear therefore that hole and electron trapping is not controlled by the concentration of the dislocations shown by this etching technique. This, however, does not exclude the possibility of other physical defects such as stacking faults or dislocations in another system being the controlling factors.

A study was also made of the carrier lifetime through a horizontal section in the crystal as it is an established fact that crystal

strain varies across the crystal cross section. The variation of hole lifetime as function of position is shown in Figure 7. We conclude

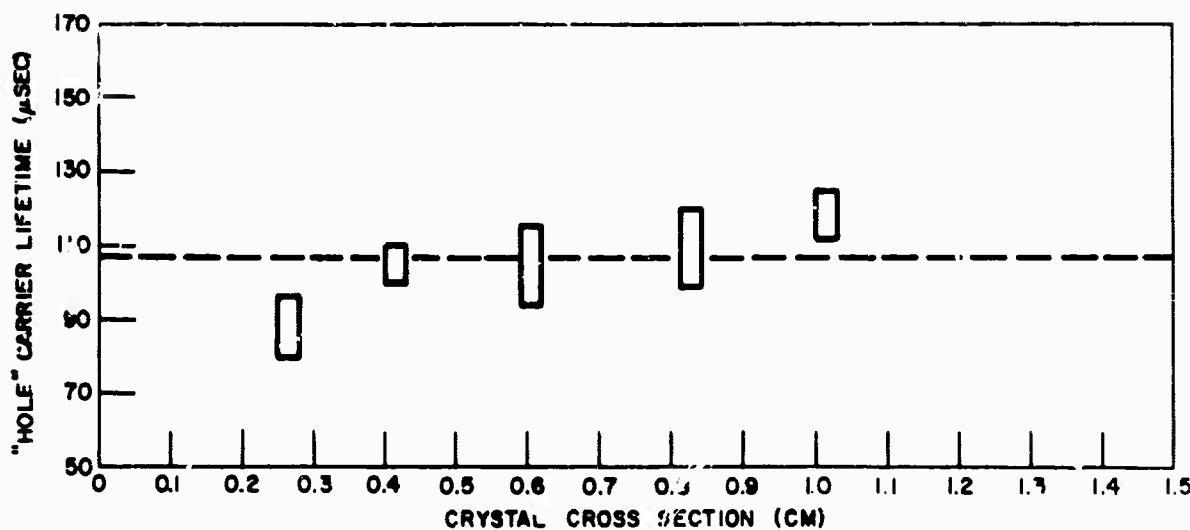


FIGURE 7. Variation of "Hole" Lifetime Through Crystal Cross Section.

from this graph that there is no significant effect of position of crystal in cross section. Only 3 electron lifetimes were measured corresponding to the first 3 points from the left and these gave lifetimes of 50, 56-58, 50-52  $\mu$ s respectively and hence also appear insensitive to position.

A study was also made of the effect of varying the exposed surface area of a large crystal by masking the crystal surface. A linear variation of pulse height with area was obtained (Figure 8) but the mobility of the charge carrier was found to increase slightly, Table III, as the area increased indicating the existence of an edge effect.

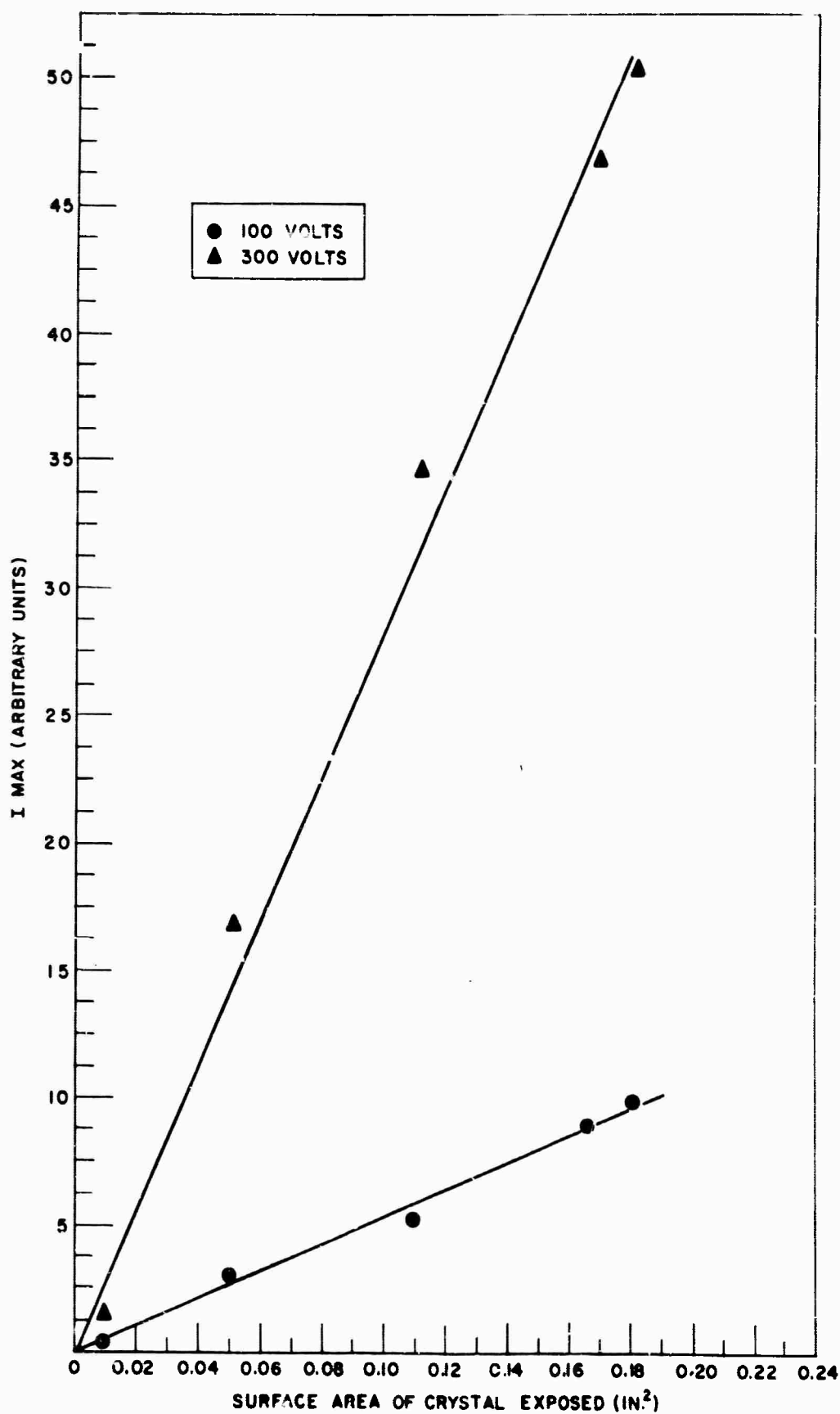


FIGURE 8. Variation of Photocurrent Pulse Height with Surface Area Illuminated.

B2130-T-11

TABLE III

VARIATION OF DRIFT TIME WITH SURFACE AREA OF CRYSTAL EXPOSED

APPLIED VOLTAGE VOLTS	SURFACE AREA, sq. in. =	DRIFT TIME - $\mu$ s ( $\propto 1/\mu$ )			
		0.012	0.049	0.110	0.196
100		~ 300-350	300	280	280
200		160	150	140	140
300		100-110	100	90	90

Another interesting point is the apparent decrease in mobility along the boule only in the case of the hole mobility which decreases from about  $0.75 \text{ cm}^2 \text{ sec}^{-1} \text{ v}^{-1}$  to  $\sim 0.6 \text{ cm}^2 \text{ sec}^{-1} \text{ v}^{-1}$ . This indicates the segregation of a shallow trapping impurity which has a segregation coefficient near  $R = 1$ . This effect was not observed in the case of the electron mobility. The variations in quoted mobilities are due to errors in measuring the thickness of the crystal as the mobility is a function of the (thickness)<sup>2</sup>.

It is planned to grow another crystal using identical purification procedures but ensuring that the crystal is held in the melt for a minimum period of time at a temperature which does not exceed the melting point by more than 20C°. A similar series of experiments will be performed in addition to self-diffusion measurements.

## 2. STUDIES ON VAPOR-GROWN ANTHRACENE CRYSTALS

In the previous report some data were presented on growth and carrier lifetimes of vapor-grown crystals. A considerable amount of effort has since been devoted to improving these crystals in size, purity and crystal perfection and a more detailed report of this activity will now be given.

A brief description of the apparatus was given previously<sup>(8)</sup>.

The material used in this set of experiments had a minimum purification of 100 zone passes in a zone refiner with a zone length/total charge length  $\sim 10-20$  thus ensuring the ultimate purification under these conditions. In the first series of crystals the purified material was introduced into the crystal growing vessel (a modified cuvette) in air and was subsequently evacuated at  $10^{-6}$  mm Hg for at least 2 hours before

sealing off under a small ambient gas pressure. Because of the severe trapping experienced in these crystals the purification and transfer process was changed to a semi-microcombination tube assembly similar to that used in the preparation of melt-grown crystal and is shown schematically in Figure 9. Here the material was zone refined then sublimed directly into crystal growing vessels after breaking the breakseal and evacuating to  $10^{-5}$  mm Hg. Ambient gas was subsequently introduced to the required pressure and the vessels sealed and removed. Several vessels were made up containing material of identical purity and under the same ambient gas. In this way the effect on the other growth parameters was studied.

In all cases the crystals were initiated by nucleating seed crystals at a supersaturation of  $\sim 100\%$  ( $10^{\circ}\text{C}$  below the ambient temperature of the oven). Normally several seeds were formed but these were subsequently boiled off by holding the heat leak at a temperature slightly above ambient until only one seed remained. The crystals were grown at ambient temperatures of  $120$ - $145^{\circ}\text{C}$  under initial supersaturations of  $10$ - $20\%$  ( $1$  to  $2.5^{\circ}\text{C}$  below ambient temperature).

The parameters that were varied were as follows.

- 1) Ambient growth temperature.
- 2) Initial supersaturation causing growth.
- 3) The ambient gas and its pressure.
- 4) The effect of growth in white light (room light) or red light ( $\lambda > 500 \text{ m}\mu$ ).
- 5) Purification procedure.

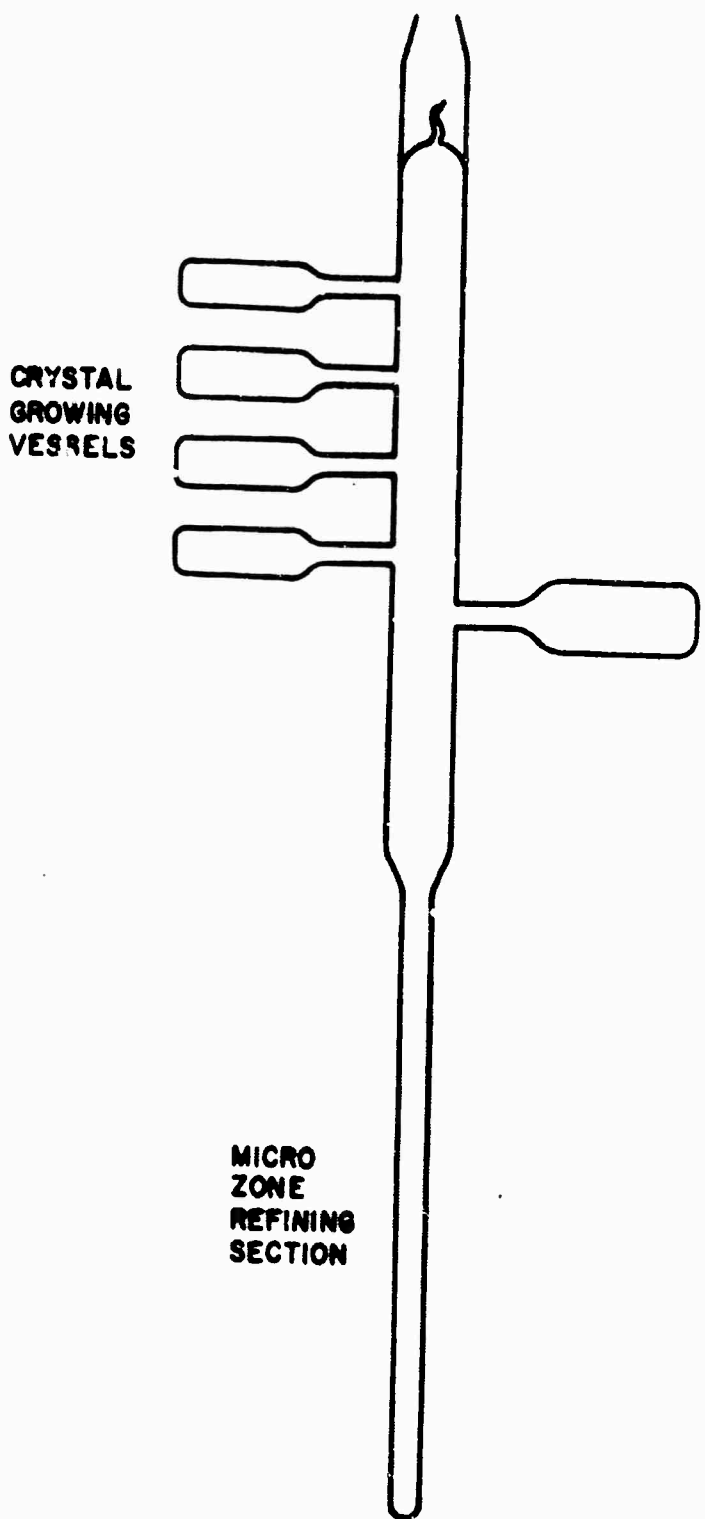


**FIGURE 9. Semimicro Combination Tube Assembly For Purification and Transfer of Material in an Inert Atmosphere.**

The crystals obtained under these growth conditions were examined for purity and perfection by studying the hole carrier lifetimes obtained in pulsed photocurrent transient measurements and dislocation structure obtained by the fuming sulfuric acid etching technique. The complete collection of results obtained to date are included in Table IV.

Conclusions which can be drawn from these experiments are as follows:

1. It is essential to purify the starting material using a combination tube technique though this alone does not guarantee a crystal with low trap densities (see VG12C).
2. Ambient inert gas pressures of 2 mm Hg and under are required for crystals of high purity and large size. Crystal VG7 for example gave a large number of very small crystals. It was also noted that very high vacuum also led to multicrystal formation if the conditions were not carefully controlled.
3. The carrier lifetime appeared independent of growth temperature or supersaturation though it was noted that in any group of crystals those grown under red light gave the longest lifetimes.
4. The carrier lifetime was independent of the measured dislocation density which in turn gave no correlation with growth temperature, ambient gas or purification procedure.
5. In the crystals in which a break in the photocurrent transient could be observed, the mobility of the holes was  $\sim 0.7 \text{ cm}^2 \text{ sec}^{-1} \text{ v}^{-1}$ , i.e. identical with that found for melt-grown crystals indicating that the impurities present did not act as shallow hole traps. In the case

TABLE IV  
PHOTOCURRENT TRANSIENT DATA FOR VAPOR-GROWN CRYSTALS

<u>Crystal Symbol</u>	<u>Carrier Lifetime, <math>\tau</math> <math>\mu</math>s</u>	<u>Dislocation density <math>\text{cm}^{-2}</math></u>	<u>Growth Temp. <math>^{\circ}\text{C}</math></u>	<u>Growth Atmosphere</u>	<u>Light Conditions</u>
VG2	20	$1-3.5 \times 10^5$	140	1 mm Purgon	White
VG3	30	$1 \times 10^5$	141	$5 \times 10^{-6}$ mm Hg	White
VG4	16-18 Air 15-17 Purgon	$1.5 \times 10^5$	140	1 mm Purgon	White
VG5	31-32 Purgon	$0.2-10 \times 10^5$	140	1 mm Purgon	White
VG6	20-24	$5 \times 10^5$	141	1 mm Purgon	White
VG7	NO CRYSTAL		141	100 mm Purgon	White
VG8	15	$4-8 \times 10^5$	141	10 mm Purgon	White
VG9	220 Air	$2-5 \times 10^5$	120	1 mm Purgon	Red
VG10A	30-70 Purgon 60 Air	$7 \times 10^5$	122	1 mm Purgon	White
VG10B	60-65 Purgon 55 Air	—	142.5	1 mm Purgon	White
VG10D	30-40 Purgon 30-35 Air	$9-10 \times 10^5$	144	1 mm Purgon	White
VG11A	135-150 Purgon 100-120 Air	—	142	1 mm Helium	White
VG11B	80 Purgon 55 Air	$5-16 \times 10^5$	134	1 mm Helium	Red
VG11C	50 Purgon 50 Air	$2-3 \times 10^5$	138	1 mm Helium	White
VG12A	65-70 Air	$3.5 \times 10^5$	141	2 mm Helium	White
VG12B	105-120 Air	$10 \times 10^5$	141	2 mm Helium	Red
VG12C	30-50 Air	$1-3 \times 10^5$	120	2 mm Helium	White
VG12D	100-110 Air	$1-3 \times 10^5$	140	$5 \times 10^{-6}$ mm Hg.	Red

of the electron pulses severe trapping prevented mobility measurements.

6. It was thought that traces of oxygen might be introduced into the growing vessels when they were pressurized to their growing conditions. To test this the VG12 series of crystals were zone refined under an ambient pressure of 40 cm helium so that any traces of oxygen would be scavenged out by the zone refining process. The breakseal was then broken and the system pumped down to the required pressure (1 mm Hg) without introducing any further amount of inert gas and sealed off. This procedure, however, does not appear to have improved the purity.

7. There appears to be no correlation between crystals which had identical purity when the growing vessels were filled i.e. crystals of the series VG10, VG11, VG12. Hence it appears that impurities must be introduced during the handling and growth procedure.

8. In no case has a crystal been obtained with lifetime comparable to pure melt-grown crystals. Hence in this respect this method of growth must be considered inferior.

### 3. DISLOCATION ETCHING STUDIES

Some further studies have been made on anthracene crystals.

It has been shown<sup>(9)</sup> that the crystallographic directions for the long and short axes of the pits obtained on etching with fuming sulfuric acid are the opposite of what we recently reported. This occurred because wrongly oriented crystals were used in this determination. This means that the crystallographic faces being developed on etching belong to the (11 L) family and not the (21 L) as was previously suggested. In order to determine L interference micrographs have been taken of an etched surface to determine the pit depth (See Figure 10). These photographs



FIGURE 10. Interference Micrograph of Anthracene Etched with Fuming Sulfuric Acid on (001) Plane.

show that pits of size  $70 \mu \times 50 \mu$  are only of the order of  $1-2 \mu$  deep which gives  $L$  a value in the range 10-20. This represents a most unusual etch plane. This micrograph was taken on a Reichert Microscope using a Watson 8 mm interference objective with a sodium filter.

#### DISLOCATION DECORATION

Further attempts have been made to prove that the etch pits obtained are dislocations. An attempt has been made to use a dislocation decoration technique similar to that of diffusing gold into alkali halides.

In the case of anthracene we tried to diffuse tetracene into the crystal hoping that it would enter preferential along dislocations.

The rationale behind this experiment was as follows. When a small quantity of tetracene (1 part in  $10^5$ ) is added to anthracene, the anthracene fluorescence is suppressed and tetracene fluorescence of high efficiency appears<sup>(10)</sup>. As the concentration of tetracene increases to  $3 \times 10^{-4}$  moles/mole, the tetracene fluorescence is more than 100 times as intense. Hence by illuminating the crystal at the anthracene absorption edge ( $400 \mu\text{m}$ ), and microscopically observing the crystal surface through a filter with a cut-off at  $500 \mu\text{m}$ , only the tetracene fluorescence at  $470-580 \mu\text{m}$  would be observed. If sufficient diffusion had taken place in the region of the dislocation, then either a point source of light or a narrow ribbon of light would be observed.

To date two such diffusion runs have been attempted. In the first several pieces of cleaved melt- and vapor-grown anthracene crystals were co-annealed with some powdered tetracene in sealed glass ampoules under a pressure of  $10^{-6}$  mm Hg for 48 hours at  $180^\circ\text{C}$ . In the

second the crystals were sealed under 13 mm Hg of argon and annealed at 180°C for 257 hours.

In neither case could any sign of decoration be detected although in some cases some substructure could be observed which is believed due to microcracks in the crystals.

These observations do not rule out the possibility of the etch pits being due to dislocations but only that either the solubility of tetracene in anthracene is extremely low or that much longer anneals near the melting point will be needed to show up this structure.

An interesting observation was made on these crystals, however, in that crystals which had been cleaved immediately prior to annealing exhibited different surface effects than "aged" cleaved surfaces. Freshly cleaved surfaces gave only the blue fluorescence of pure anthracene with no sign of the green tetracene fluorescence whereas "aged" surfaces gave only tetracene fluorescence. This indicated that the tetracene had penetrated into the anthracene lattice as an epitaxial deposit of tetracene would not give the intense fluorescence observed, pure tetracene being a very inefficient fluorescer. Presumably the explanation is that the aged surface has an oxidized layer which on formation must break up the surface and facilitate the tetracene penetration. A further proof of this point is included in the section on electron microscopy.

#### 4. ELECTRON MICROSCOPY

In an effort to gain further insight into the physical structure of organic crystals we have turned to electron microscopy.

This is a standard technique for studying the defect structure of metallic and inorganic solids but has been little used for organic molecular crystals due to their high volatility and relatively low melting point.

Initial attempts to study anthracene were made on ultra-thin sections ( $< 1000 \text{ \AA}$ ) of anthracene crystals obtained by stripping a crystal surface with scotch tape and examining them in a JEM7 electron microscope. These crystals, however, suffered severe evaporation when subjected to the electron beam and no useful studies could be made. A possible improvement in this technique would be to introduce a cold stage to the microscope but this was not feasible at the time.

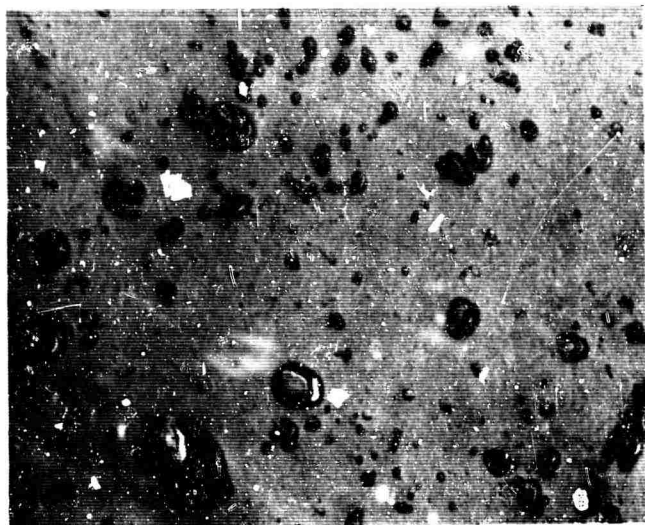
The second technique used was to prepare replicas of crystal surfaces using standard electron microscopy methods. Crystals of anthracene were taken from several sources, commercially supplied crystals, melt-grown crystals and vapor-grown crystals and replicas were made of "aged" cleaved surfaces i.e. cleaved crystals which had been standing in air more than a week, freshly cleaved surfaces, i.e. surfaces cleaved immediately prior to replication and surfaces etched with fuming sulfuric acid.

The replication technique used initially was to mount the crystals on a glass slide using paraffin wax, evacuate in a vacuum evaporation unit and evaporate on a thin film,  $\sim 500 \text{ \AA}$  of a water soluble material (Vickawet) followed by another coating of silicon monoxide. These films were subsequently floated off the crystal by gradually immersing in a bowl of distilled water. The silicon monoxide film was then picked up by immersing a microscope grid under the film and removing from the water. The grids were allowed to dry then re-evacuated and a thin coating of tungsten oxide  $\sim 500 \text{ \AA}$  evaporated on at an angle of about

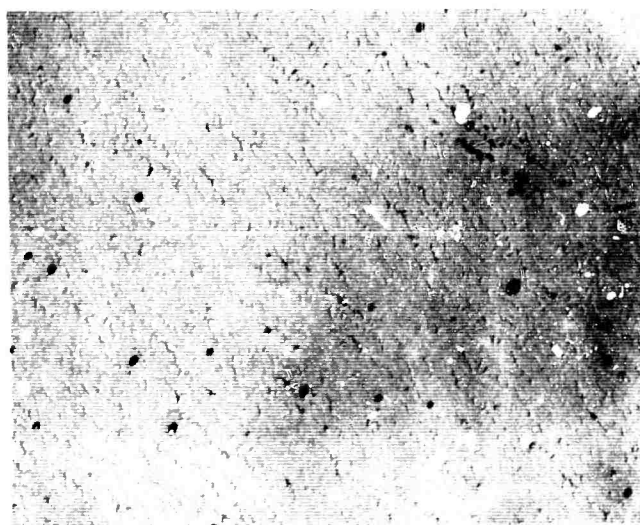
45° i.e. the crystals were shadowed so that humps and depressions could be distinguished. The most difficult part of this technique was removing the silicon monoxide layer from the crystal and there were only a few crystals where this was accomplished successfully. Several other solvents were tried but with no success. No replicas could be obtained with the etched surfaces.

Figure 11a and b show replicas of "aged" and freshly cleaved surfaces of Harshaw crystals. The difference in the surfaces is quite apparent. The circular pits in Figure 11b have a density of  $\sim 2 \times 10^5 \text{ cm}^{-2}$  which roughly corresponded with the density of etch pits obtained using fuming sulfuric acid. The parallel ribbon pattern, however, is unique to this crystal and cannot be observed in Figure 11a. It is possible that they represent evaporation etching of dislocations lying in the ab plane. If this were so, then their density would be at least an order of magnitude greater than those perpendicular to the ab plane. Figure 11a shows that the surface is much rougher possibly due to chemical attack by oxygen which may form a barrier layer preventing the evaporation observed in Figure 11b.

Figure 12 shows the surface replica obtained from a vapor-grown crystal. This is yet again quite different from those in Figure 11. Shallow pits are again obvious but their density is  $\sim 5 \times 10^7 \text{ cm}^{-2}$  which is two orders of magnitude greater than the etch pit density. Due to the difficulty of removing this film from the crystal there is some doubt about its validity and several crystals are being re-examined at present.



(a)



(b)

**FIGURE 11. Electron Micrograph Replicas of Cleaved Surfaces of Commercially Supplied Anthracene Single Crystal. Mag. X 4,600 a) "Aged Surface b) Freshly Cleaved Surface.**



FIGURE 12. Electron Micrograph Replica of Freshly Cleaved Vapor-Grown Anthracene Crystal. Mag. X 12,000.



FIGURE 13. Electron Micrograph Replica of Freshly Cleaved Melt-Grown Anthracene. Ref. 47-33. Mag. X 1,600.

Due to the difficulty of using this replication technique another method of removing the replica was used. Instead of water immersion a coating of replica solution (cellulose acetate) was placed on the silicon monoxide layer, allowed to harden then peeled off taking the replica with it. This layer was then placed on a grid and washed with refluxing acetone. Only one crystal replica has been examined by this method, a melt-grown crystal, ref. 47-33, and part of its surface is shown in Figure 13. This is an excellent example of what is presumably dislocation evaporation etching. The rows of dislocations may represent pile-ups at a boundary. Note also the layered evaporation structure. Examination of this photograph at higher magnification and assuming that the crystal was shadowed at  $\sim 45^\circ$  indicates that the step height between layers is of the order of 150 Å. The dark spots appearing on the photograph are simply spots of tungsten oxide which appeared due to overheating another region of the replica.

Further work is in progress to check that these replicas give a true representation of the crystal surface structures.

While studying these replicas it was found that thin flakes of anthracene were sometimes stripped from the crystal surface and gave excellent electron diffraction patterns. Attempts are being made to index these patterns and a fuller discussion will be given in the next report. These photographs are interesting in that as well as indicating possible structural faults e.g. twinning and stacking faults they yield some information on electron scattering by thermal molecular motion in the lattice. Figure 14 shows a micrograph of such a crystal. Here several strained regions in the crystal can be observed. The cause of these strained regions, however, is



FIGURE 14. Electron Micrograph of Anthracene Crystal. Mag. X 90,000.

not yet uniquely known and it must be remembered that each side of the crystal is coated with  $\sim 500 \text{ \AA}$  of silicon monoxide and tungsten oxide respectively, the effect of which is not known.

Work in this field is being continued and it is hoped that the result will be a much clearer understanding of the physical structure of organic crystals.



P. J. Reucroft  
Manager  
Chemistry Laboratory



A. R. McGhie  
Post-Doctoral Associate

Approved:



M. M. Labes  
Sr. Consultant  
Chemistry Department

REFERENCES

- (1) P. J. Reucroft, H. K. Kevorkian, M. M. Labes, Diffusion in Organic Crystals. II., *J. Chem. Phys.* 44, 4415, 1966.
- (2) J. N. Sherwood and D. J. White, paper presented at Organic Crystal Symposium, Chicago, May 1965.
- (3) Semi-Annual Technical Report B2130-T-9, 1 October 1965 - 31 March 1966.
- (4) G. Castro, Ph.D. Thesis 1965, Univ. of California.
- (5) D. C. Hoesterey and G. M. Letson, *J. Phys. Chem. Solids* 24, 1609, 1963.
- (6) H. Herington, "Zone Melting of Organic Compounds", Wiley 1963, p. 14.
- (7) G. J. Sloan, *Molecular Crystals* 1, 161, 1966.
- (8) Semi-Annual Technical Report B2130-T-10, 1 April 1966 - 30 September 1966.
- (9) N. C. Corke, A. A. Kawada and J. N. Sherwood, *Nature* 213, 62, 1967.
- (10) F. R. Lipsett, "Energy Transfer in Polyacene Solid Solutions", A guide to the literature to the end of 1956, N.R.C, Ottawa 1957.